

Spontaneous CP-violation in the Simplest Little Higgs Model and its Future Tests at e^+e^- Colliders: the Scalar Sector

Ying-nan Mao ^{1,*}

¹ *Center for Future High Energy Physics & Theoretical Physics Division,
Institute of High Energy Physics, Chinese Academy of Sciences, Beijing 100049, China*

(Dated: June 26, 2022)

We proposed the possibility of spontaneous CP-violation in the simplest little Higgs model. The CP-symmetry is spontaneously broken after the pseudoscalar field requires its vacuum expected value. The scalars with different CP-charge mix with each other hence they become CP-mixing state. The existence of CP-violation in scalar sector can be confirmed through measuring a nonzero K (see the text). Facing all constraints, especially the electric dipole moment of electron, this model is still alive. We discussed the tests on this model at future e^+e^- colliders. For the recent allowed regions, 5σ discovery for CP-violation in the scalar sector is possible when the extra scalar is lighter than about 70 GeV at CEPC with 5 ab^{-1} luminosity. If the extra scalar is heavier, more simulation studies are needed. At the end of the discussion section, we also briefly discussed the tests on this model at LHC for the case with a heavy extra scalar.

arXiv:1703.10123v1 [hep-ph] 29 Mar 2017

* maoyan@ihep.ac.cn

I. INTRODUCTION

A 125 GeV standard model (SM) like Higgs boson [1, 2] was discovered by the ATLAS and CMS collaborations [3] in 2012. It implies the success of the SM, however, physics beyond the SM (BSM) is still attractive. The little Higgs (LH) framework which contains a class of models was proposed by Arkani-Hamed *et al.* [4] to solve the little hierarchy problem. As a type of composite models [5], the LH models contain a global symmetry which is spontaneously broken at a high scale $f \gg v$ where $v = 246$ GeV is the vacuum expected value (VEV) of the Higgs field. The Higgs boson is treated as a pseudo-Nambu-Goldstone boson corresponding to one of the broken generators thus it can be naturally light [4]. The simplest little Higgs (SLH) model [6] is one of such kind of models which has the minimal extended scalar sector. In the SLH model, the global symmetry breaking $[\text{SU}(3) \times \text{U}(1)]^2 \rightarrow [\text{SU}(2) \times \text{U}(1)]^2$ happens at high scale f , and the gauge group $\text{SU}(3) \times \text{U}(1)$ breaks to the electro-weak (EW) gauge group $\text{SU}(2)_L \times \text{U}(1)$ at the same scale [6]. In the CP-conserving case, the SLH model contains two scalars [6] that one is a SM-like Higgs boson and the other is a pseudoscalar which can be at the EW scale or even lighter [7].

CP-violation was discovered in 1964 through the $K_L \rightarrow \pi\pi$ rare decay process [8]. More CP-violation effects have been discovered in K and B meson sectors [2]. The Kobayashi-Maskawa (K-M) mechanism [9] is successful to explain all the measured CP-violation effects [2]. However, it is still necessary to search for new CP-violation sources, since the SM with K-M mechanism itself cannot generate large enough matter-antimatter asymmetry in the universe [2, 10–12]. In the extensions of the SM, there may be additional sources of CP-violation. For example, if we add more complex scalar singlets or doublets, there may be CP-violation in scalar sector [13] which can lead to a CP-mixing Higgs boson¹. In some of these models with CP-violation, the Lagrangian is CP-conserved and CP-violation is only generated from complex vacuum thus we say the CP-symmetry is spontaneously broken. This mechanism was proposed by Lee in 1973 [15] as the first kind of two-Higgs-doublet model (2HDM) [13]. Moreover, spontaneous CP-violation is also a possible solution of the

¹ For the 125 GeV Higgs boson, LHC measurements preferred a CP-even one and excluded a CP-odd one at over 3σ level through the final distribution of $h \rightarrow ZZ^* \rightarrow 4\ell$ decay assuming no CP-violation in the Higgs interactions [14]. However, a CP-mixing Higgs boson is still allowed since the contribution from pseudoscalar component should be loop suppressed.

strong CP problem [16], and it may also have further connection with lightness of the Higgs boson [17].

In the composite framework, spontaneous CP-violation in the scalar sector can also occur. For example, in the SO(6)/SO(5) model (which is equivalent to the SU(4)/Sp(4) model as the next-to-minimal composite model) [18], there are two scalars like the SLH model, and CP-violation can be spontaneously induced when the pseudoscalar field acquires VEV. Similarly, in the littlest Higgs model, spontaneous CP-violation can be induced through the same mechanism [19, 20]. In this paper, we will propose the spontaneous CP-violation SLH model through the realization of the same mechanism.

Recently, Mao *et al.* proposed a model-independent method to measure the CP-violation effects in scalar sector at e^+e^- colliders [21]. If there are two scalars, like in the SLH model, the effective tree level interaction between scalars and Z boson should be written as

$$\mathcal{L}_{\text{tree}} = \frac{g^2 v}{4c_{\theta_W}^2} Z_\mu Z^\mu (c_1 h_1 + c_2 h_2) + \frac{c_{12} g}{2c_{\theta_W}} Z_\mu (h_1 \partial^\mu h_2 - h_2 \partial^\mu h_1) \quad (1)$$

where $h_{1,2}$ denote the two scalars, g is the weak coupling constant, and θ_W is the EW mixing angle ². The product

$$K \equiv c_1 c_2 c_{12} \quad (2)$$

is a useful quantity to measure CP-violation in the scalar sector [21, 23]. $K \neq 0$ is a sufficient (but not necessary) condition of CP-violation in the scalar sector. Based on this, we can try to search for the three tree-level vertices $h_{1,2}ZZ$ and $h_1 h_2 Z$ to confirm CP-violation in the scalar sector.

In this paper, the 125 GeV Higgs boson is denoted as h_1 , and the other scalar is denoted as h_2 . This paper is organized as following: in section II we build the SLH model with spontaneous CP-violation and obtain the domain interactions; in section III we consider the experimental constraints, especially in the scalar sector; in section IV we discuss the future tests on this model at e^+e^- colliders; and in section V we present our conclusions and further discussions.

² In this paper, we denote $s_\alpha \equiv \sin \alpha$, $c_\alpha \equiv \cos \alpha$, and $t_\alpha \equiv \tan \alpha$ for any angle α . For the $h_1 h_2 Z$ interaction, if we consider a physical process, the final matrix element must be equivalent to the formalism written in (1) where the two terms have coefficients opposite to each other, no matter in linear or nonlinear realized model [22]. We don't consider the $h_i W^+ W^-$ interactions in this paper in details.

II. MODEL CONSTRUCTION AND THE INTERACTIONS

The SLH model contains two scalar triplets $\Phi_{1,2}$ which transform as $(\mathbf{3}, \mathbf{1})$ and $(\mathbf{1}, \mathbf{3})$ respectively under the global $[\text{SU}(3) \times \text{U}(1)]^2$ transformation [6, 7, 24]. At a scale $f \gg v$, $[\text{SU}(3) \times \text{U}(1)]^2$ breaks to $[\text{SU}(2) \times \text{U}(1)]^2$ and generate ten Nambu-Goldstone bosons, of which eight should be eaten by massive gauge bosons during spontaneous gauge symmetry breaking $\text{SU}(3) \times \text{U}(1) \rightarrow \text{SU}(2)_L \times \text{U}(1) \rightarrow \text{U}(1)_{\text{em}}$. Two physical scalars are finally left thus the nonlinear realized scalar triples can be written as

$$\Phi_1 = e^{it_\beta \Theta} \begin{pmatrix} \mathbf{0}_{1 \times 2} \\ f c_\beta \end{pmatrix}, \quad \Phi_2 = e^{-i\Theta/t_\beta} \begin{pmatrix} \mathbf{0}_{1 \times 2} \\ f s_\beta \end{pmatrix}; \quad (3)$$

where β is a mixing-angle between the scalar triplets and

$$\Theta \equiv \frac{1}{f} \left(\frac{\eta \mathbb{I}_{3 \times 3}}{\sqrt{2}} + \begin{pmatrix} \mathbf{0}_{2 \times 2} & \phi \\ \phi^\dagger & 0 \end{pmatrix} \right). \quad (4)$$

Here written in the interaction eigen-state, $\phi \equiv (G^+, (v_h + h + iG^0)/\sqrt{2})^T$ is the usual Higgs doublet ³ and η is a pseudoscalar.

In the SLH model without CP-violation, h and η are also their mass eigen-states. h can acquire its mass through loop correction [6, 7] which breaks the global $[\text{SU}(3) \times \text{U}(1)]^2$ explicitly, however, an accidental global $\text{U}(1)$ symmetry remains a massless η unless a $\Phi_1^\dagger \Phi_2$ term (called μ -term) is added into the scalar potential [7]. To generate spontaneous CP-violation, the additional terms dependent on η in the potential are

$$\delta V = -\mu^2 \Phi_1^\dagger \Phi_2 + \epsilon \left(\Phi_1^\dagger \Phi_2 \right)^2 + \text{H.c.} \quad (5)$$

$m_\eta \sim \mu \lesssim \mathcal{O}(v)$ and $\epsilon \sim \mathcal{O}(m_\eta^2/f^2) \lesssim \mathcal{O}(v^2/f^2)$ to keep the spontaneous EW symmetry breaking ⁴. Denoting $\alpha \equiv v/(\sqrt{2}f s_\beta c_\beta)$, when

$$\mu^2 < 4\epsilon f^2 |s_\beta c_\beta c_\alpha|, \quad (6)$$

³ In the SLH model, the VEV of h field is modified to $v_h = v \left(1 - \left(t_\beta^2 - 1 + t_\beta^{-2} \right) v^2/12f^2 + \mathcal{O}(v^4/f^4) \right)$ [7].

⁴ The second term in (5) will break the stability of EW scale during radiative correction since it hardly breaks the accidental global $\text{U}(1)$ which remains η massless. However, spontaneous EW symmetry breaking requires $\epsilon \sim \mathcal{O}(m_\eta^2/f^2) \lesssim \mathcal{O}(v^2/f^2)$ which means the EW scale should still be stable under the power counting of the scale f .

$\langle \eta \rangle = 0$ would become an unstable vacuum thus η acquires a VEV

$$v_\eta \equiv \langle \eta \rangle = \pm \sqrt{2} f s_\beta c_\beta \arccos \left(\frac{\mu^2}{4\epsilon f^2 s_\beta c_\beta c_\alpha} \right) \quad (7)$$

which means CP-symmetry is spontaneously broken. From now on, we choose “+” in the equation above for simplify. Denoting $\xi \equiv v_\eta / (\sqrt{2} f s_\beta c_\beta)$, it can be as large as $\mathcal{O}(1)$. The mass term for scalars is

$$\mathcal{L}_{\text{mass}} = -\frac{1}{2} (\eta, h) \begin{pmatrix} 4\epsilon f^2 c_\alpha^2 s_\xi^2 & \epsilon f^2 s_{2\alpha} s_{2\xi} \\ \epsilon f^2 s_{2\alpha} s_{2\xi} & M^2 \end{pmatrix} \begin{pmatrix} \eta \\ h \end{pmatrix} \quad (8)$$

where M should be close to 125 GeV. η and h mix with each other that the mass eigen-states are no longer CP eigen-states. The mass eigen-states

$$\begin{pmatrix} h_1 \\ h_2 \end{pmatrix} = \begin{pmatrix} c_\theta & -s_\theta \\ s_\theta & c_\theta \end{pmatrix} \begin{pmatrix} h \\ \eta \end{pmatrix} \quad (9)$$

with the mixing angle

$$\theta = \frac{1}{2} \arctan \left(\frac{2\epsilon f^2 s_{2\alpha} s_{2\xi}}{M^2 - 4\epsilon f^2 c_\alpha^2 s_\xi^2} \right). \quad (10)$$

The masses of the scalars are

$$m_{1,2} = \sqrt{\frac{M^2 + 4\epsilon f^2 c_\alpha^2 s_\xi^2}{2} \pm \left(\frac{M^2 - 4\epsilon f^2 c_\alpha^2 s_\xi^2}{2} c_{2\theta} + \epsilon f^2 s_{2\alpha} s_{2\xi} s_{2\theta} \right)}. \quad (11)$$

For $f \gg v$, to the leading order of v/f , the coefficients in (1) are [24, 25, 36]

$$c_1 = c_\theta \left(1 - \frac{v^2}{4f^2} \left(t_\beta^2 + \frac{1}{t_\beta^2} - t_{\theta_W}^2 (2 - t_{\theta_W}^2) \right) \right); \quad (12)$$

$$c_2 = s_\theta \left(1 - \frac{v^2}{4f^2} \left(t_\beta^2 + \frac{1}{t_\beta^2} - t_{\theta_W}^2 (2 - t_{\theta_W}^2) \right) \right); \quad (13)$$

$$c_{12} = \frac{v}{\sqrt{2}f} \left(t_\beta - \frac{1}{t_\beta} \right). \quad (14)$$

The trilinear interaction between h_1 and h_2 can be parameterized as

$$\mathcal{L}_S = -\frac{1}{2} \lambda_{122} h_1 h_2 h_2 - \frac{1}{2} \lambda_{211} h_2 h_1 h_1. \quad (15)$$

The couplings are

$$\lambda_{122} = \frac{\sqrt{2}\epsilon f s_{2\alpha}}{s_{2\beta}} (3c_{2\xi} - 1); \quad (16)$$

$$\lambda_{211} = \frac{\sqrt{2}\epsilon f s_{2\xi}}{s_{2\beta}} (3c_{2\alpha} - 1). \quad (17)$$

In the SLH model, the fermions are in $\mathbf{3}$ or $\mathbf{3}^*$ representation of SU(3) group that there must be an extra lepton and an extra heavy quark in each generation [24, 25]. In the SLH model with spontaneous CP-violation, according to [7, 24, 25], the SM fermions' couplings to scalars $h_{1,2}$ are given as

$$\mathcal{L}_f = - \sum_f \frac{m_f}{v} \bar{f}_L (c_{1,f} h_1 + c_{2,f} h_2) f_R + \text{H.c.} \quad (18)$$

where to the leading order we have

$$c_{1,U_i} = c_{1,D_i}^* = c_\theta - i s_\theta c_{12}, \quad c_{2,U_i} = c_{2,D_i}^* = s_\theta + i c_\theta c_{12}; \quad (19)$$

$$c_{1,Q_j} = i s_\theta \frac{v (c_{2\beta} - c_{2\theta_i})}{\sqrt{2} f s_{2\beta}}, \quad c_{2,Q_j} = -i c_\theta \frac{v (c_{2\beta} - c_{2\theta_i})}{\sqrt{2} f s_{2\beta}}. \quad (20)$$

where $U(D)_i$ denote the SM up (down) type quarks, Q_i denote the heavy quarks, and θ_i denote the right-handed mixing angle between heavy quarks and the SM quarks in the same generation. We don't discuss the Yukawa couplings carefully here. More details of the physics in the fermion sector of this model are going to appear in a forthcoming paper [26].

III. RECENT CONSTRAINTS ON THE MODEL

We have assumed $m_1 = 125$ GeV as the discovered scalar. However, theoretically m_2 is almost free. It can be as large as $\mathcal{O}(v)$ due to EW symmetry breaking, and it may also be hidden below the EW scale if μ^2 and ϵ are very small. At different mass region, the phenomenology are quite different so that most of the discussions must be divided into different parts according to m_2 . The main constraints come from collider experiments on direct searches and Higgs signal strengths, EW precision measurements [27, 28], and electric dipole moments (EDM) of electron and neutron [29–31]. Here we don't focus on the constraints from flavor physics.

A. Constraints from Colliders Searches

For a new light h_2 , the constraints come from LEP direct searches through Zh_2 and $h_1 h_2$ associated production which gave [32–34]

$$c_2 \lesssim (0.1 - 0.2), \quad (\text{for } m_2 \sim (15 - 80) \text{ GeV}); \quad (21)$$

$$c_{12} \lesssim (0.4 - 0.7), \quad (\text{for } m_2 \sim (10 - 50) \text{ GeV}). \quad (22)$$

at 95% C.L assuming all scalars decay to $b\bar{b}$ final state. The constraint on c_{12} is not strict in this model because it is suppressed by v/f . For a new heavy h_2 , there is almost no constraint from LHC direct searches since the production cross section $\sigma_{gg \rightarrow h_2}$ is suppressed by $(v/f)^2$.

For a light h_2 , if $m_2 < m_1/2$, there are also constraints through h_1 rare decay processes, including $h_1 \rightarrow 2h_2$ and $h_1 \rightarrow Z^{(*)}h_2$. The recent LHC results still allow the exotic branching ratio $\text{Br}_{\text{exo}} \lesssim (0.2 - 0.3)$ at 95% C.L. assuming Higgs couplings are SM-like [35]. The rare decay widths are [2]

$$\Gamma_{h_1 \rightarrow 2h_2} = \frac{\lambda_{122}^2}{32\pi m_1} \sqrt{1 - \frac{4m_2^2}{m_1^2}}; \quad (23)$$

$$\Gamma_{h_1 \rightarrow Z^{(*)}h_2} = \frac{3m_Z \Gamma_Z c_{12}^2}{8\pi^2 m_1^2 v^2} \int_0^\pi d\theta \sin^3 \theta \int_0^{(m_1 - m_2)^2} ds^* \frac{m_2^2 s^* p^*}{(s^* - m_Z^2)^2 + m_Z^2 \Gamma_Z^2} \cdot \frac{\beta^{*2}}{1 - \beta^{*2}}. \quad (24)$$

Here in (24), s^* is the invariant mass square of final states from Z^* ; and

$$p^* = \frac{\sqrt{(m_1^2 - (m_2 - \sqrt{s^*})^2)(m_1^2 - (m_2 + \sqrt{s^*})^2)}}{2m_1}, \quad (25)$$

$$\beta^* = \frac{m_1 p^*}{p^{*2} + \sqrt{(p^{*2} + m_2^2)(p^{*2} + s^*)}}, \quad (26)$$

are the momentum of h_2 in the center-of-mass frame and the relative velocity between h_2 and Z^* separately. (24) is suitable for both Z on-shell and off-shell cases. When $m_2 < m_1 - m_Z$, the dominant contribution comes from on-shell Z (with $s^* = m_Z^2$) and thus (24) can be reduced to

$$\Gamma_{h_1 \rightarrow Zh_2} = \frac{m_1^3 c_{12}^2}{16\pi^2 v^2} \mathcal{F}\left(\frac{m_Z^2}{m_1^2}, \frac{m_2^2}{m_1^2}\right)^3 \quad (27)$$

where the function

$$\mathcal{F}(x, y) = \sqrt{1 + x^2 + y^2 - 2x - 2y - 2xy}. \quad (28)$$

In (23) we consider only the case both two h_2 in the final state are on-shell, because h_2 is estimated very narrow (for such light h_2 , $\Gamma_2 \lesssim \mathcal{O}(\text{keV})$) that the decay width decreased quickly when h_2 becomes off-shell. In Figure 1 we show the exotic decay widths $\Gamma_{h_1 \rightarrow Z^{(*)}h_2}$ and $\Gamma_{h_1 \rightarrow 2h_2}$ for different couplings c_{12} and c_2 . The exotic decay width $\Gamma_{h_1 \rightarrow 2h_2}$ is very sensitive to c_2 and m_2 , but it is not sensitive to f and β in most regions⁵. In Figure 2 and

⁵ In the limit $f \rightarrow \infty$, λ_{122} is independent on f and β .

FIG. 1: Exotic decay widths $\Gamma_{h_1 \rightarrow Z^{(*)} h_2}$ and $\Gamma_{h_1 \rightarrow 2h_2}$. In the left figure, the width depend only on the coupling $c_{12} \equiv v(t_\beta - 1/t_\beta)/(\sqrt{2}f)$, while in the right figure, the width is sensitive to c_2 and m_2 . In the left figure, when $m_2 > 34$ GeV, the Z boson in final state must be off-shell thus the decay width falls quickly when m_2 grows. In the right figure, we fix $f = 6$ TeV and $t_\beta = 3$, but numerical results show that it is not sensitive to f and β .

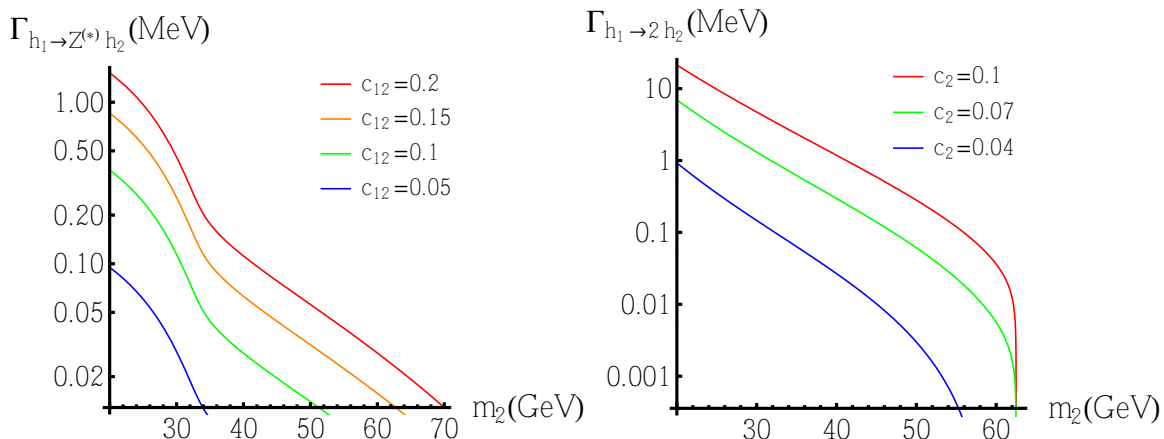


FIG. 2: Exotic decay branching ratios in SLH model with spontaneous CP-violation with fixed $f = 6$ TeV. From left to right we choose $c_{12} = 0.2, 0.15, 0.1, 0.05$, respectively.

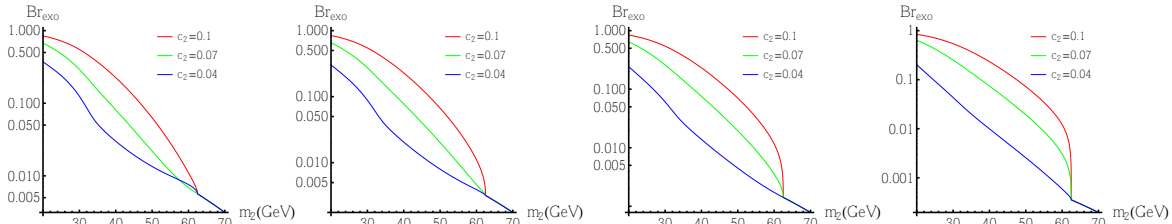


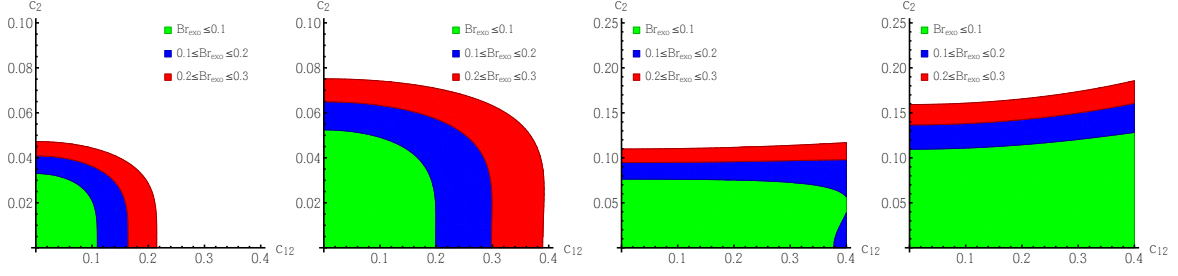
Figure 3 we show the exotic branching ratios for different m_2 , c_2 and c_{12} fixing $f = 6$ TeV. For $m_2 \lesssim m_1 - m_Z = 34$ GeV, $h_1 \rightarrow Zh_2$ is open with an on-shell Z boson that c_{12} is strictly constrained together with c_2 ; while for $m_1 - m_Z < m_2 < m_1/2$, $h_1 \rightarrow Z^* h_2$ decays only through an off-shell Z boson thus there is no strict constraint on c_{12} ; and for $m_2 > m_1/2$, there are no constraints from Higgs rare decay processes.

B. Constraints from Oblique Parameters

The recent global fits for oblique parameters S and T are [28]

$$\begin{aligned}
 S &= 0.05 \pm 0.11, \quad T = 0.09 \pm 0.13, \quad R_{ST} = +0.90 \quad (\text{leaving } U \text{ free}); \\
 S &= 0.06 \pm 0.09, \quad T = 0.10 \pm 0.07, \quad R_{ST} = +0.91 \quad (\text{fixing } U = 0).
 \end{aligned}
 \tag{29}$$

FIG. 3: Exotic decay branching ratios distribution in c_2 - c_{12} plane with fixed $f = 6$ TeV. From left to right we choose $m_2 = 20$ GeV, 30 GeV, 40 GeV, 50 GeV, respectively.



R_{ST} here means the correlation between S and T parameters. Dominant contributions to S and T parameters from the scalar sector in this model are given by [6, 13, 36, 37]

$$\delta S \simeq \frac{2s_{\theta_W}^2 v^2}{\alpha_W f^2} - \frac{v^2}{18\pi f^2} \left(t_\beta^2 - 1 + \frac{1}{t_\beta^2} \right) \left(c_1^2 \ln \frac{m_1}{\Lambda} + c_2^2 \ln \frac{m_2}{\Lambda} \right); \quad (30)$$

$$\delta T \simeq \frac{v^2}{8\alpha_W f^2} (1 - t_{\theta_W}^2)^2 + \frac{v^2}{8\pi c_{\theta_W}^2 f^2} \left(t_\beta^2 - 1 + \frac{1}{t_\beta^2} \right) \left(c_1^2 \ln \frac{m_1}{\Lambda} + c_2^2 \ln \frac{m_2}{\Lambda} \right). \quad (31)$$

Here $\alpha_W \equiv g^2/(4\pi) = \alpha_{\text{em}}/s_{\theta_W}^2$ and $\Lambda \sim 4\pi f$ is the cut-off scale. It is similar to the case without CP-violation. The 95% C.L. lower limit of f modifies in the region (4 – 7) TeV assuming $|s_\beta c_\beta| \gtrsim 0.1$ [36] which corresponds to a constraint $|c_{12}| \lesssim 0.2$ ⁶ at 95% C.L. This result is not sensitive to m_2 when $c_2 \sim s_\theta \ll 1$. The constraint is stricter in large ($\gg 1$) or small ($\ll 1$) t_β regions, because in those regions, additional contributions to oblique parameters from neutral scalars are larger according to (30) and (31).

C. EDM Constraints

A fermion f 's EDM is defined through the effective interaction [29]

$$\mathcal{L}_{f,\text{EDM}} = -\frac{i}{2} d_f \bar{f} \sigma_{\mu\nu} \gamma^5 f F^{\mu\nu} \quad (32)$$

which breaks both P and CP symmetries. In the SM, CP-violation comes only from complex CKM matrix that the leading contributions to the EDMs of electron and neutron arise at four- and three-loop level respectively. It is estimated that [29]

$$d_{e,\text{SM}} \sim 10^{-38} e \cdot \text{cm}, \quad d_{n,\text{SM}} \sim 10^{-32} e \cdot \text{cm}, \quad (33)$$

⁶ The final constraints are similar if we use the HEPfit results [38] instead of the GFitter results [28].

which are far below the recent experimental constraints [30, 31]

$$|d_e| < 8.7 \times 10^{-29} e \cdot \text{cm}, \quad |d_n| < 3.0 \times 10^{-26} e \cdot \text{cm}, \quad (34)$$

both at 90% C.L.

The two-loop Barr-Zee type diagrams [39] give dominant contribution to the fermion EDM as [40–42]

$$\begin{aligned} \frac{d_f}{e} = & \sum_{i=1,2} \frac{2\sqrt{2}G_F\alpha_{\text{em}}Q_fm_f}{(4\pi)^3} \left(c_i \text{Im}(c_{i,f}) \left(\left(6 + \frac{m_i^2}{m_W^2} \right) f \left(\frac{m_W^2}{m_i^2} \right) + \left(10 - \frac{m_i^2}{m_W^2} \right) g \left(\frac{m_W^2}{m_i^2} \right) \right) \right. \\ & \left. - 12 \sum_{F=t,Q_j} Q_F^2 \left(\text{Im}(c_{i,F}) \text{Re}(c_{i,f}) g \left(\frac{m_F^2}{m_i^2} \right) + \text{Im}(c_{i,f}) \text{Re}(c_{i,F}) f \left(\frac{m_F^2}{m_i^2} \right) \right) \right), \quad (35) \end{aligned}$$

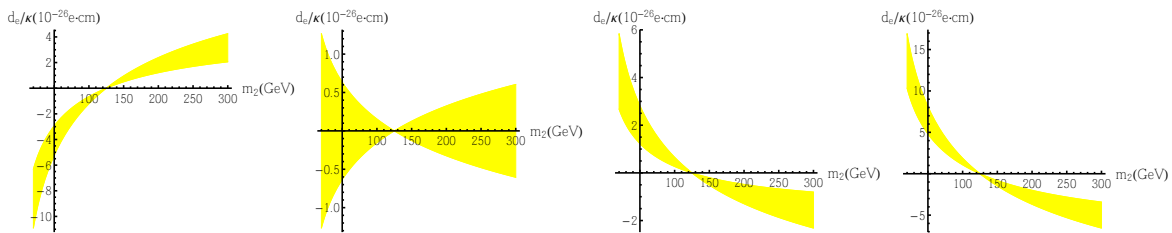
where Q_j denote extra heavy quarks as in (20) and the loop integration functions are

$$f(z) \equiv \frac{z}{2} \int_0^1 dx \frac{1 - 2x(1-x)}{x(1-x) - z} \ln \frac{x(1-x)}{z}; \quad (36)$$

$$g(z) \equiv \frac{z}{2} \int_0^1 dx \frac{1}{x(1-x) - z} \ln \frac{x(1-x)}{z}. \quad (37)$$

For electron, its EDM can be completely described by (35). Using the results (19) and (20), to the leading order, we have $d_e \propto \kappa \equiv c_\theta s_\theta v/f \simeq c_1 c_2 v/f$ whose typical value is of $\mathcal{O}(10^{-3})$. In Figure 4 we show d_e/κ with different β .

FIG. 4: d_e/κ with $t_\beta = 0.3, 1, 2, 5$ respectively from left to right. The yellow bands appear due to the variation of the right-handed mixing angles θ_j . The results are not sensitive to the heavy quark mass thus we fix them at 10 TeV during numerical calculations.



The main constraints appear at the large or small m_2 regions. The constraints on κ are sensitive to β , however, assuming $t_\beta > 1$, we have that d_e/K depends weakly on t_β in large t_β region ⁷ where $K = \kappa(t_\beta - 1/t_\beta)/\sqrt{2}$ is defined in (2). So the constraints on K depend weakly

⁷ The same results appear in the large $1/t_\beta$ region if $t_\beta < 1$.

on β if t_β is not close to 1. For a light h_2 , for example, $m_2 \sim (20 - 70)$ GeV as discussed above, we have $K \lesssim (0.2 - 1) \times 10^{-2}$ which is sensitive to m_2 but not sensitive to β and θ_i . K is just the quantity to measure CP-violation effects in the scalar sector. Comparing with the results in Figure 3, in the low mass region, EDM constraints are stricter than the constraints from rare decay processes. Similarly, for a heavy h_2 with its mass $m_2 \sim (200 - 300)$ GeV, we have $K \lesssim (0.5 - 1) \times 10^{-2}$ if t_β is not close to 1. In the region $m_2 \sim (70 - 200)$ GeV, $K \sim 10^{-2}$ is usually allowed which means the constraint is not strict. Moreover, $|d_e|$ vanishes when $m_1 = m_2$ because of the cancelation between the contributions from h_1 and h_2 separately⁸. For $t_\beta \sim 1$, $t_\beta \sim 1/t_\beta$ thus $K \sim 0$. The SM particles' contributions to the electron EDM are all proportional to K so that the dominant contributions come from extra quarks if $t_\beta \sim 1$. In this case, $\kappa \sim 10^{-2}$ is always allowed according to the second plot in Figure 4.

For neutron, there are three types of operators contribute to its EDM and the effective interaction can be written as [29, 40]

$$\mathcal{L}_{n,\text{EDM}} = -\frac{i}{2} \sum_{q=u,d} \left(d_q \bar{q} \sigma^{\mu\nu} \gamma^5 q F_{\mu\nu} + g_s \tilde{d}_q \bar{q}_i \sigma^{\mu\nu} \gamma^5 (t^a)_{ij} q_j G_{\mu\nu}^a \right) - \frac{w}{3} f^{abc} G_{\mu\nu}^a G_{\rho}^{\nu,b} \tilde{G}^{\mu\rho,c} \quad (38)$$

where t^a and f^{abc} are the generation and structure constant for color SU(3) group. The quark EDM d_q can be calculated from (35), quark color EDM \tilde{d}_q and the coefficient of Weinberg operator [43] w are both generated at two-loop level as [40, 43]

$$\begin{aligned} \tilde{d}_q &= - \sum_{\substack{i=1,2 \\ F=t,Q_j}} \frac{G_F \alpha_s m_q}{\sqrt{2}(2\pi)^3} \left(\text{Im}(c_{i,F}) \text{Re}(c_{i,q}) g \left(\frac{m_F^2}{m_i^2} \right) + \text{Im}(c_{i,q}) \text{Re}(c_{i,F}) f \left(\frac{m_F^2}{m_i^2} \right) \right), \quad (39) \\ w &= \sum_{i=1,2} \frac{\sqrt{2} G_F \alpha_s}{(4\pi)^3} \text{Im}(c_{i,t}) \text{Re}(c_{i,t}) \mathcal{W} \left(\frac{m_t^2}{m_i^2} \right); \quad (40) \end{aligned}$$

both at EW scale μ_W . The heavy quarks' contributions to Weinberg operator are negligible and the function

$$\mathcal{W}(x) = x^2 \int_0^1 du \int_0^1 dv \frac{(1-v)(uv)^3}{((1-u)(1-v) + xv(1-uv))^2}. \quad (41)$$

We consider the running effects following the appendix of [40], and obtain the neutron EDM at hadron scale μ_H [17]

$$\frac{d_n}{e} \simeq \frac{m_d(\mu_H)}{m_d(\mu_W)} \left(0.63 \frac{d_d}{d} + 0.73 \cdot \tilde{d}_d \right) + \frac{m_u(\mu_H)}{m_u(\mu_W)} \left(-0.16 \frac{d_u}{e} + 0.19 \cdot \tilde{d}_u \right) + (9.8 \text{ MeV}) w. \quad (42)$$

⁸ As another comprehension, when $m_1 = m_2$, the scalar mixing angle θ is arbitrary and we can always choose $\theta = 0$ which means extra CP-violation in the scalar sector disappears facing the degeneration of scalar masses

In this model, if the parameter choices satisfy the electron EDM constraint, the typical numerical result on neutron EDM show that $|d_n| \lesssim 10^{-27} e \cdot \text{cm}$ which is still below the recent experimental limit thus it cannot give further constraints.

IV. FUTURE TESTS AT e^+e^- COLLIDERS

To test CP-violation in the scalar sector, $K \equiv c_1 c_2 c_{12}$ is a key observable [21]. In this model, c_1 is assumed ~ 1 thus the measurements on c_2 and c_{12} are important. For a light h_2 with its mass $m_2 \lesssim 100$ GeV, it can be produced at a Higgs factory, like CEPC [44] or TLEP [45], with $\sqrt{s} = (240 - 250)$ GeV. c_2 can be measured only through Zh_2 associated production; and c_{12} can be measured through $h_1 h_2$ associated production or $h_1 \rightarrow Z^{(*)} h_2$ rare decay. The cross sections for $e^+e^- \rightarrow Z^* \rightarrow Zh_2/h_1 h_2$ are given as [34, 46]

$$\sigma_{Zh_2} = \frac{\pi \alpha_{\text{em}}^2 s (8s_{\theta_W}^4 - 4s_{\theta_W}^2 + 1) \cdot c_2^2}{96(s - m_Z^2)^2 s_{\theta_W}^4 c_{\theta_W}^4} \left(\mathcal{F}^3 \left(\frac{m_Z^2}{s}, \frac{m_2^2}{s} \right) + \frac{12m_Z^2}{s} \mathcal{F} \left(\frac{m_Z^2}{s}, \frac{m_2^2}{s} \right) \right); \quad (43)$$

$$\sigma_{h_1 h_2} = \frac{\pi \alpha_{\text{em}}^2 s (8s_{\theta_W}^4 - 4s_{\theta_W}^2 + 1) \cdot c_{12}^2}{96(s - m_Z^2)^2 s_{\theta_W}^4 c_{\theta_W}^4} \mathcal{F}^3 \left(\frac{m_1^2}{s}, \frac{m_2^2}{s} \right). \quad (44)$$

The function \mathcal{F} is defined in (28). For a heavy h_2 , a Higgs factory doesn't have enough \sqrt{s} thus we need other colliders, such as ILC [47] with $\sqrt{s} = (350 - 500)$ GeV or CLIC with larger \sqrt{s} [48, 49]. For this case, c_2 can be measured through vector boson fusion (VBF) or Zh_2 associated production; and c_{12} can be measured through $h_1 h_2$ associated production or $h_2 \rightarrow Z^{(*)} h_1$ decay.

At CEPC with $\sqrt{s} = 250$ GeV and 5 ab^{-1} luminosity, the typical 5σ discovery bound for an exclusive Higgs rare decay branching ratio is around $\mathcal{O}(10^{-3})$ [44, 50]. Thus using $h_1 \rightarrow Z^{(*)}(\rightarrow f\bar{f})h_2$ rare decay, For low m_2 region (for example, $m_2 \lesssim m_1 - m_Z = 34$ GeV), $c_{12} \sim \mathcal{O}(10^{-2})$ can be discovered at 5σ level at CEPC with 5 ab^{-1} luminosity. For larger m_2 thus Z boson is off-shell, if $\text{Br}_{h_1 \rightarrow Z^* h_2} \gtrsim 10^{-3}$, the required boundary for c_{12} increases with the increasing of m_2 , and reach $\mathcal{O}(0.1)$ when $m_2 = 70$ GeV.

The sensitivities for c_2 and c_{12} depend weakly on m_2 in low mass region (for example, $m_2 \lesssim 70$ GeV) if we directly measure the cross sections $\sigma_{Zh_2, h_1 h_2}$ through the recoil-mass method [44, 51, 52] according to the simulation study in [21]. The inclusive measurement can determine the couplings and hence their product K in a model-independent way [21]. However, with the inclusive measurements, the 5σ discovery bounds are too large facing

the EDM constraints in section III for low m_2 region, though the “ p_T balance” method [53] is helpful to reduce backgrounds including photons. But, if we give up the inclusiveness and choose an exclusive decay channel, such as $h_2 \rightarrow b\bar{b}$, the background will become quite smaller and it would be easier to discover these processes. For example, using the $h_2 \rightarrow b\bar{b}$ decay channel, the 5σ discovery bounds would become $c_2 \sim (4 - 5) \times 10^{-2}$ and $c_{12} \sim (8 - 11) \times 10^{-2}$ [21, 54] which are about half of the boundaries through inclusive measurements. Besides these, precision measurement on $\text{Br}_{h_1 \rightarrow 2h_2}$ is also helpful to give a cross-check on the measurement of c_2 .

Comparing with the constraints in section III, in the whole $m_2 \lesssim 70\text{GeV}$ region, it is possible to discover both c_2 and c_{12} at 5σ level at CEPC in the allowed parameter regions and hence confirm CP-violation in the scalar sector. When $m_2 \lesssim (50 - 60)\text{GeV}$, to measure c_{12} , the rare decay channel $h_1 \rightarrow Z^{(*)}h_2$ is more effective than the production channel $e^+e^- \rightarrow Z^* \rightarrow h_1h_2$. Using these two channels, if both processes are discovered at over 5σ level, the corresponding $K \gtrsim (1 - 4) \times 10^{-3}$ which is still allowed by the EDM constraint $K \lesssim (2 - 10) \times 10^{-3}$ for $m_2 \sim (20 - 60)\text{GeV}$. If $m_2 \gtrsim 60\text{GeV}$, the associated production channel $e^+e^- \rightarrow Z^* \rightarrow h_1h_2$ is more effective on discovering c_{12} .

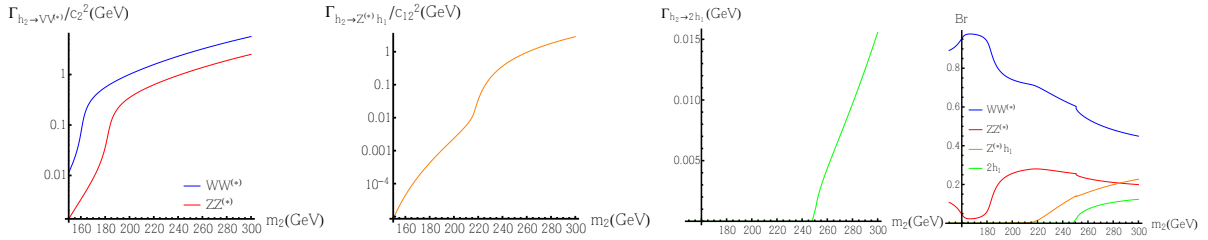
When m_2 is close to Z peak, for example, $m_2 \sim (80 - 100)\text{GeV}$, for $e^+e^- \rightarrow Zh_2/h_1h_2$ channel, large ZZ/Zh_1 background will be difficult to reduce thus the sensitivity will become worse. We need more analysis in this region. For heavier h_2 but $m_2 < m_1$, 5σ discovery bound for c_2 will reach around 0.1, however, $\sigma_{h_1h_2}$ will decrease quickly with an increasing m_2 since it is close to the h_1h_2 associated production threshold at CEPC. For the upper limit $c_2 \sim 0.2$ from oblique parameter constraints, the sensitivity will drop from about $(4 - 5)\sigma$ to zero when m_2 increases from about 100 GeV to $\sqrt{s} - m_1 = 125\text{GeV}$. But in this region, EDM constraints becomes weak due to the cancelation between the contributions from two scalars, so that $c_2 \sim 0.1$ and $c_{12} \sim 0.2$ are still allowed in this model.

If m_2 is heavier, we cannot test this model at CEPC. If we still want to test it at e^+e^- colliders, we need a larger \sqrt{s} . For $m_2 \sim (150 - 300)\text{GeV}$, at ILC with $\sqrt{s} = 500\text{GeV}$, the dominant channel to measure c_2 is through Zh_2 associated production and VBF production [55]. Both the two cross sections are suppressed by a factor ⁹ $c_2^2 \sim 10^{-2}$ thus $\sigma_{Zh_2+\text{VBF}} \sim$

⁹ In the SLH model, the modifications for $h_iW^+W^-$ and h_iZZ vertices are different to $\mathcal{O}(v^2/f^2)$. If we ignore this tiny difference, we can choose them the same c_2 .

$\mathcal{O}(0.1 - 1)$ fb [46–48, 55, 56]. With $\mathcal{O}(\text{ab}^{-1})$ luminosity, totally $\mathcal{O}(10^2 - 10^3)$ events can be collected to measure c_2 . Similarly, for $h_1 h_2$ associated production, we can collect events number of the same order. The dominant decay channels are $h_2 \rightarrow WW^{(*)}$, $ZZ^{(*)}$, and $Z^{(*)}h_1$. If $m_2 > 2m_1 = 250$ GeV, $h_2 \rightarrow 2h_1$ decay channel is also open. In Figure 5 we show the decay widths and branching ratios [55–58] for these decay channels of h_2 . Numerical

FIG. 5: Partial decay widths and branching ratios for $h_2 \rightarrow WW^*$, ZZ^* , Z^*h_1 , and $2h_1$. Fermion final states are ignorable in this mass region. The first two figures showed the ratio between the decay widths and the square of couplings for the three dominant decay channels. In the last two figures, we fix $c_2 = c_{12} = 0.1$ and $f = 6$ TeV.



results show that the decay width $\Gamma_{h_2 \rightarrow 2h_1}$ is sensitive to c_2 and m_2 , but not sensitive to c_{12} and f . At this benchmark point, $\text{Br}_{h_2 \rightarrow 2h_1}$ can reach about 10% which is still not dominant. When $m_2 = 300$ GeV, Γ_2 will reach $\mathcal{O}(10^2)$ MeV. In the whole mass region, the largest decay channel is $h_2 \rightarrow WW^{(*)}$. More simulation studies are still needed to confirm what the sensitivity would reach for this model at future e^+e^- colliders, for example, with the typical couplings $c_2 \sim c_{12} \sim 0.1$, and typical luminosity $\mathcal{O}(\text{ab}^{-1})$.

V. CONCLUSIONS AND DISCUSSIONS

In this paper we propose the possibility of spontaneous CP-violation in the SLH model. Through adding a new interaction term in the scalar potential, the pseudoscalar field η can acquire its nonzero VEV thus CP-symmetry is spontaneously broken. The two scalars with different CP-charge will mix with each other thus they are no longer CP eigenstates. Experimentally, CP-violation in the scalar sector can be confirmed if a quantity $K \neq 0$.

We consider the recent constraints on this model, especially in the scalar sector. For most mass region besides $m_2 \simeq m_1$, the dominant constraint comes from the EDM of electron. It usually requires $K \lesssim 10^{-2}$, and for $m_2 \sim 20$ GeV, the EDM constraint is about $K \lesssim 2 \times 10^{-3}$. When $m_2 \sim m_1$, the contributions from different scalars are cancelled by each other that

this constraint becomes weak. There are no further constraints from neutron EDM in this model. In the low mass region $m_2 < m_1/2$, this model should also face the constraints from h_1 rare decay. It requires $c_2 \lesssim (0.04 - 0.07)$ for $m_2 \sim (20 - 30)$ GeV. The oblique parameter constraints are sensitive to f and β , but not sensitive to m_2 or c_2 . It requires $c_{12} \lesssim 0.2$ in the whole mass region, which is the most strict constraint for $m_2 \gtrsim (20 - 30)$ GeV. In summary, this model is still alive facing all these constraints.

We also discuss the future tests for this model at future e^+e^- colliders. If $m_2 \lesssim m_1$, it can be tested at CEPC with $\sqrt{s} = 250$ GeV. In this mass region, c_2 can be measured through Zh_2 associated production channel. c_{12} can be measured through $h_1 \rightarrow Z^{(*)}h_2$ decay if $m_2 \lesssim (50 - 60)$ GeV, while it should be measured through h_1h_2 associated production for heavier h_2 . For $m_2 \lesssim 70$ GeV, nonzero c_2 and c_{12} are both possible to be discovered at 5σ level and hence $K \neq 0$ can be confirmed. While in the $t_\beta \sim 1$ region, c_{12} cannot be measured thus CP-violation in the scalar sector is difficult to confirm. There is also a blind mass region, m_2 close to Z peak, which would be difficult to measure these couplings because of large backgrounds which are difficult to reduce. If $m_2 > m_1$, CEPC beam energy is not large enough and we need colliders with larger \sqrt{s} .

In this paper, we focus on the future tests at e^+e^- colliders. However, besides e^+e^- colliders, we can also try to test this model for large $m_2 (\gtrsim m_Z + m_1 = 216 \text{ GeV})$ region at LHC which is running. It is possible to confirm CP-violation in the scalar sector if both decay channels $h_2 \rightarrow VV$ and Zh_1 are discovered as proposed in [17, 21]. Different from e^+e^- colliders, at LHC, the dominant production channel for h_2 is gluon fusion that the cross section is suppressed by a factor $(v/f)^2$. However, an enhancement from extra heavy quark loops also exceeds that $\sigma_{gg \rightarrow h_2}$ can reach $(3 - 4) \times 10^2 \cdot c_{12}^2$ pb at LHC with $\sqrt{s} = 14$ TeV in the large t_β or t_β^{-1} region if the right-handed mixing between the extra quark and the corresponding SM quark are small [56–59]. With 3 ab^{-1} luminosity, based on the analysis by CMS Collaboration [60], if $c_{12} \sim 0.1$, the significance for $h_2 \rightarrow ZZ$ channel is possible to reach 5σ in the whole $m_2 \sim (220 - 300)$ GeV region when $c_2 \gtrsim 0.02$; while the significance for $h_2 \rightarrow Zh_1$ may reach about $(3 - 5)\sigma$ for $m_2 \sim (250 - 300)$ GeV if $c_2 \lesssim 0.05$ ¹⁰. If $c_{12} \sim 0.15$, $c_2 \gtrsim 0.02$ can lead to a 5σ discovery of $h_2 \rightarrow ZZ$ channel as well; however, the discovery of

¹⁰ That's because a large c_2 will lead to large partial width for $h_2 \rightarrow VV$ channels which cause a smaller branching ratio for $h_2 \rightarrow Zh_1$

$h_2 \rightarrow Zh_1$ is easier, it can be discovered at 3σ for the whole $m_2 \sim (250 - 300)$ GeV region if $c_2 \lesssim 0.08$, while the significance can increase to 5σ if $c_2 \lesssim 0.06$. These numerical results above are based on t_β away from 1 which means a large $c_{12} \sim \mathcal{O}(0.1)$. If $t_\beta \sim 1$, the cross section would be only $\mathcal{O}(10 \text{ fb})$ which cannot be discovered at LHC.

Acknowledgement

We thank Shi-ping He, Fa-peng Huang, Gang Li, Ling-xiao Xu, Chen Zhang, and Shou-hua Zhu for helpful discussions.

-
- [1] The ATLAS and CMS Collaborations, Phys. Rev. Lett. 114, 191803, (2015).
 - [2] K. A. Olive *et al.* (Particle Data Group), Chin. Phys. C 38, 090001 (2014); Chin. Phys. C 40, 100001 (2016).
 - [3] The ATLAS Collaboration, Phys. Lett. B 716, 1 (2012); The CMS Collaboration, Phys. Lett. B 716, 30 (2012).
 - [4] N. Arkani-Hamed, A. G. Cohen, and H. Georgi, Phys. Lett. B 513, 232 (2001); N. Arkani-Hamed, A. G. Cohen, E. Katz, and A. E. Nelson, J. High Energy Phys. 07, 034 (2002); N. Arkani-Hamed, A. G. Cohen, E. Katz, A. E. Nelson, T. Gregoire, and J. G. Wacker, J. High Energy Phys. 08, 021 (2002); M. Schmaltz and D. Tucker-Smith, Ann. Rev. Nucl. Part. Sci. 55, 229 (2005).
 - [5] D. B. Kaplan and H. Georgi, Phys. Lett. B 136, 183 (1984).
 - [6] D. E. Kaplan and M. Schmaltz, J. High Energy Phys. 10, 039 (2003); M. Schmaltz, J. High Energy Phys. 08, 056 (2004).
 - [7] K. Cheung and J. Song, Phys. Rev. D 76, 035007 (2007); K. Cheung, J. Song, P. Tseng, and Q.-S. Yan, Phys. Rev. D 78, 055015 (2008).
 - [8] J. H. Christenson, J. W. Cronin, V. L. Fitch, and R. Turlay, Phys. Rev. Lett. 13, 138 (1964).
 - [9] M. Kobayashi and T. Maskawa, Prog. Theor. Phys. 49, 652 (1973).
 - [10] P. A. R. Ade *et al.* (The Planck Collaboration), Astron. Astrophys. 571, A16 (2014).
 - [11] D. E. Morrissey and M. J. Ramsey-Musolf, New J. Phys. 14, 125003 (2012).

- [12] A. G. Cohen, D. B. Kaplan, and A. E. Nelson, Phys. Lett. B 263, 86 (1991); Annu. Rev. Nucl. Part. Sci. 43, 27 (1993); J. Shu and Y. Zhang, Phys. Rev. Lett. 111, 091801 (2013).
- [13] G. C. Branco, P. M. Ferreira, L. Lavoura, M. N. Rebelo, M. Sher, and J. P. Silva, Phys. Rep. 516, 1 (2012).
- [14] The CMS Collaboration, Phys. Rev. D 89, 092007 (2014); The ATLAS Collaboration, Report No. ATLAS-CONF-2015-008.
- [15] T. D. Lee, Phys. Rev. D 8, 1226 (1973); Phys. Rep. 9, 143 (1974).
- [16] J. E. Kim and G. Garosi, Rev. Mod. Phys. 82, 557 (2010); S. M. Barr, Phys. Rev. Lett. 53, 329 (1984).
- [17] Y.-N. Mao and S.-H. Zhu, Phys. Rev. D 90, 115024 (2014); Phys. Rev. D 94, 055008 (2016); Phys. Rev. D 94, 059904 (2016, erratum); Y.-N. Mao, PhD Thesis (Peking University, 2016).
- [18] B. Gripaios, A. Pomarol, F. Riva, and J. Serra, J. High Energy Phys. 04, 070 (2009).
- [19] Z. Surujon and P. Uttayarat, Phys. Rev. D 83, 076010 (2011).
- [20] H. E. Haber and Z. Surujon, Phys. Rev. D 86, 075007 (2012).
- [21] G. Li, Y.-N. Mao, C. Zhang, and S.-H. Zhu, Phys. Rev. D 95, 035015 (2017).
- [22] Private discussions with Chen Zhang *et al.*, paper in prepration.
- [23] A. Méndez and A. Pomarol, Phys. Lett. B 272, 313 (1991); J. F. Gunion and H. E. Haber, Phys. Rev. D 72, 095002 (2005).
- [24] F. del Águila, J. I. Illana, and M. D. Jenkins, J. High Energy Phys. 03, 080 (2011).
- [25] T. Han, H. E. Logan, and L.-T. Wang, J. High Energy Phys. 01, 099 (2006).
- [26] Y.-N. Mao, in prepration.
- [27] M. E. Peskin and T. Takeuchi, Phys. Rev. Lett. 65, 964 (1990); Phys. Rev. D 46, 381 (1992).
- [28] M. Baak, J. Cuth, J. Haller, A. Hoecker, R. Kogler, K.Mönig, M. Schott, and J. Stelzer, Eur. Phys. J. C 74, 3046 (2014).
- [29] M. Pospelov and A. Ritz, Ann. Phys. (Amsterdam) 318, 119 (2005).
- [30] The ACME Collaboration, Science 343, 269 (2014).
- [31] C. Baker *et al.*, Phys. Rev. Lett. 97, 131801 (2006); J. M. Pendlebury *et al.*, Phys. Rev. D 92, 092003 (2015).
- [32] The ALEPH, DELPHI, L3, and OPAL Collaborations (LEP Higgs Working Group), Report No. LHWG Note/2001-04, arXiv: hep-ex/0107030.
- [33] G. Abbiendi *et al.* (ALEPH, DELPHI, L3, and OPAL Collaborations (the LEP Higgs Working

- Group)), Phys. Lett. B 565, 61 (2003).
- [34] S. Schael *et al.* (ALEPH, DELPHI, L3, and OPAL Collaborations (the LEP Higgs Working Group)), Eur. Phys. J. C 47, 547 (2006).
- [35] D. Curtin *et al.*, Phys. Rev. D 90, 075004 (2014).
- [36] J. Reuter and M. Tonini, J. High Energy Phys. 02, 077 (2013); M. Tonini, Report No. DESY-THESIS-2014-038, PhD Thesis (Universität Hamburg, 2014).
- [37] G. Marandella, C. Schappacher, and A. Strumia, Phys. Rev. D 72, 035014 (2005).
- [38] J. de Blas, M. Ciuchini, E. Franco, S. Mishima, M. Pierini, L. Reina, and L. Silvestrini, J. High Energy Phys. 12, 135 (2016).
- [39] S. M. Barr and A. Zee, Phys. Rev. Lett. 65, 21 (1990); Phys. Rev. Lett. 65, 2920 (1990, erratum).
- [40] J. Brod, U. Haisch, and J. Zupan, J. High Energy Phys. 11, 180 (2013).
- [41] T. Abe, J. Hisano, T. Kitahara, and K. Tobioka, J. High Energy Phys. 01, 106 (2014).
- [42] K. Cheung, J. S. Lee, E. Senaha, and P.-Y. Tseng, J. High Energy Phys. 06, 149 (2014).
- [43] S. Weinberg, Phys. Rev. Lett. 63, 2333 (1989); D. A. Dicus, Phys. Rev. D 41, 999 (1990); E. Braaten, C.-S. Li, and T.-C. Yuan, Phys. Rev. Lett. 64, 1709 (1990).
- [44] The CEPC-SPPC Study Group, Reports No. IHEP-CEPC-DR-2015-01, No. IHEP-TH-2015-01, and No. IHEP-EP-2015-01, http://cepc.ihep.ac.cn/preCDR/main_preCDR.pdf.
- [45] M. Bicer *et al.* (TLEP Design Study Working Group), J. High Energy Phys. 01, 164 (2014).
- [46] S. Heinemeyer and C. Schappacher, Eur. Phys. J. C 76, 220 (2016).
- [47] C. Adolphsen *et al.*, arXiv: 1306.6328; arXiv: 1306.6353; D. Asner *et al.*, arXiv: 1310.0763.
- [48] The CLIC Physics Working Group, Report No. CERN-2004-005, arXiv: hep-ph/0412251.
- [49] H. Abramowicz *et al.*, Report No. CLICDP-PUB-2016-001, arXiv: 1608.07538.
- [50] Z. Liu, L.-T. Wang, and H. Zhang, Report No. FERMILAB-PUB-16-608-T, arXiv: 1612.09284.
- [51] J. F. Gunion, T. Han, and R. Sobey, Phys. Lett. B 429, 79 (1998).
- [52] NLC ZDR Design Group and NLC Physics Working Group Collaborations, arXiv: hep-ex/9605011.
- [53] H. Li, arXiv: 1007.2999; PhD Thesis (Université de Paris-Sud, 2009), <http://hal.inria.fr/file/index/docid/430432/filename/Li.pdf>.
- [54] Private discussions with Gang Li *et al.*

- [55] ECFA/DESY LC Physics Working Group, Reports No. SLAC-REPRINT-2001-002, No. DESY-01-011, No. DESY-01-011C, No. DESY-TESLA-2001-23, No. DESY-TESLA-FEL-2001-05, and No. ECFA-2001-209, arXiv: hep-ph/0106315.
- [56] A. Djouadi, Phys. Rep. 457, 1 (2008); Phys. Rep. 459, 1 (2008).
- [57] LHC Higgs Cross Section Working Group, Reports No. CERN-2013-004 and No. FERMILAB-CONF-13-667-T, arXiv: 1307.1347;
- [58] LHC Higgs Cross Section Working Group, Report No. FERMILAB-FN-1025-T, arXiv: 1610.07922.
- [59] LHC Higgs Cross Section Working Group, Report No. CERN-2011-002, arXiv: 1101.0593.
- [60] The CMS Collaboration, Report No. CMS-PAS-FTR-13-024.